Antiferroquadrupolar Order and Rotational Symmetry Breaking in a Generalized Bilinear-Biquadratic Model on a Square Lattice

Hsin-Hua Lai, Wen-Jun Hu, Emilian M. Nica, Rong Yu, and Qimiao Si

Phys. Rev. Lett. **118**, 176401 — Published 25 April 2017

DOI: 10.1103/PhysRevLett.118.176401

Antiferroquadrupolar order and rotational symmetry breaking in a generalized bilinear-biquadratic model on a square lattice

Hsin-Hua Lai,[1] Wen-Jun Hu,[1] Emilian M. Nica,[1] Rong Yu,[2,3] and Qimiao Si[1]

[1]*Department of Physics and Astronomy & Rice Center for Quantum Materials, Rice University, Houston, Texas 77005, USA*
[2]*Department of Physics, Renmin University of China, Beijing, 100872, China*
[3]*Department of Physics and Astronomy, Shanghai Jiao Tong University, Shanghai 200240, China and Collaborative Innovation Center of Advanced Microstructures, Nanjing 210093, China*

(Dated: April 6, 2017)

The magnetic and nematic properties of the iron chalcogenides have recently been the subject of intense interest. Motivated by the proposed antiferroquadrupolar and Ising-nematic orders for the bulk FeSe, we study the phase diagram of an $S = 1$ generalized bilinear-biquadratic model with multi-neighbor interactions. We find a large parameter regime for a (π,0) antiferroquadrupolar phase, showing how quantum fluctuations stabilize it by lifting an infinite degeneracy of certain semiclassical states. Evidence for this C_4-symmetry-breaking quadrupolar phase is also provided by an unbiased density matrix renormalization group analysis. We discuss the implications of our results for FeSe and related iron-based superconductors.

Introduction— Much of the current effort in the study of the iron-based superconductors (FeSCs) is devoted to understanding the magnetism in their normal state [1, 2]. While the iron pnictides were the focus of the early effort in the FeSC field, iron chalcogenides have occupied the center stage more recently. Among them, FeSe takes a special place. In the single-layer limit, FeSe has the highest superconducting transition temperature among the FeSCs [3–6]. In bulk form, this compound is a canonical superconducting member with a very simple structure [7, 8]. It displays a typical tetragonal-to-orthorhombic structural transition, with $T_s \approx 90$ K, but, surprisingly, no Néel transition [9–16]. This is puzzling, because it differs from the standard case of the iron pnictides where the structural phase transition is accompanied by a $(\pi, 0)$ antiferromagnetic (AFM) order [17]. Several theoretical proposals attribute this unusual behavior to the frustrated magnetism among the local moments [18–20]. Two of the present authors considered a generalized bilinear-biquadratic (GBQ) model on a square lattice and proposed that an antiferroquadrupolar (AFQ) state with wave vector $(\pi, 0)$ describes the bulk FeSe [18]. This theoretical picture predicted low-energy spin excitations near $(\pi, 0)$, which has since been experimentally observed [21, 22]. It also predicted a linear-in-energy spectral weight for such low-energy spin excitations and, over a wider energy range, spin excitations near both $(\pi, 0)$ and (π, π), all of which have also been verified in recent experiments [23, 24]. More broadly, the neutron scattering measurements show that the spin spectral weight is even larger than that of the AFM state in the iron pnictides [23, 24], which provides further support for describing the magnetic properties of FeSe in terms of frustrated magnetism.

The proposed *two-sublattice* C_4-symmetry-breaking AFQ state is a novel state of matter, and systematic theoretical studies are clearly called for. Quadrupolar order *per se* in frustrated spin models has been studied before [25–35], representing an intriguing spin state that involves the ordering of spin quadrupolar moments without exhibiting a magnetic dipolar order. However, two-sublattice AFQ order such as the proposed $(\pi, 0)$ phase has not been realized before as a zero-temperature phase in such quantum-spin models, and the nature of the associated rotational symmetry breaking has not been addressed. In particular, it would be important to establish if the AFQ order is a true ground state of the GBQ model when the quantum fluctuations are fully accounted for.

In this *Letter*, we demonstrate that the $(\pi, 0)$ AFQ state is the ground state of the spin $S = 1$ GBQ model on a square lattice over an extended parameter range. We have done so by two complementary means. We first show that the AFQ order has the lowest energy for a range of parameters based on a site-factorized wavefunction [30, 31, 33, 36, 37]. From a flavor-wave analysis, we show that quantum fluctuations lift an infinite degeneracy in the ground state energy and stabilize the AFQ ground state with order at either $(\pi, 0)$ or $(0, \pi)$. Such order-from-disorder physics is analogous to what happens for the case of pure antiferromagnetic order [38, 39], although it has never before been realized for any two-sublattice AFQ order. We then show that the AFQ order is the true ground state even when the quantum fluctuations are treated fully and in an unbiased way, using the density matrix renormalization group (DMRG) method [40, 41]. Finally, from a symmetry-based treatment, we establish that the AFQ order parameter does not couple to bilinear fermions, thereby demonstrating the consistency of the $(\pi, 0)$ AFQ order with the single-electron spectrum observed in FeSe. We stress that both the problem we address, and the analysis we carry through, are new to the present work. We note in passing that the stabilization of the C_4-symmetry-breaking AFQ by the quantum fluctuation effects not only provides an intriguing mechanism for the nematic order in the normal state of the iron chalcogenide FeSe, but also suggests the possible realization of such a "hidden order" phase in cold atom systems tuned away from the SU(N>2) symmetric point, in which bilinear-biquadratic couplings can be realized [42].

Generalized Bilinear-Biquadratic Model— We consider the GBQ model on a two-dimensional square lattice,

$$H = \sum_{i,\delta_n} \left[J_n \mathbf{S}_i \cdot \mathbf{S}_j + K_n \left(\mathbf{S}_i \cdot \mathbf{S}_j \right)^2 \right], \qquad (1)$$

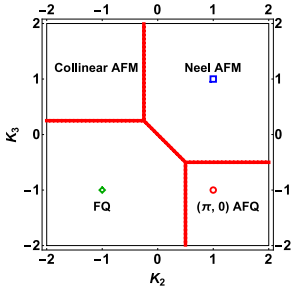

FIG. 1. (Color online) The phase diagram derived from the site-factorized wavefunction studies, as a function of K_2 and K_3. We have fixed $J_1 = J_2 = 1/4$, and $K_1 = -1$. Collinear AFM represents an antiferromagnet with wave vectors $(\pi, 0)/(0, \pi)$, and Néel AFM with (π, π). The $(\pi, 0)$ AFQ corresponds to the antiferro-quadrupolar phase, which has an infinite degeneracy that is to be lifted by quantum fluctuations. FQ corresponds to the ferroquadrupolar state. The red open circle, green open diamond, and blue open square are three parameter points for which the DMRG results will be presented.

where $j = i + \delta_n$, and δ_n connects site i and its nth nearest neighbor sites with $n = 1,\ 2,\ 3$. The couplings J_n and K_n are the bilinear and biquadratic couplings between the nth nearest neighbor spins. The importance of the biquadratic couplings K_n (along with the bilinear couplings J_n) has been suggested both from an analysis of the inelastic neutron-scattering spectra in the iron pnictides [43] as well as from *ab initio* studies [44]. The large magnitude inferred for the biquadratic coupling is compatible with the expectation for multi-orbital models in the bad-metal regime [45]. We expect that K_n will contain not only a nearest-neighbor term ($n = 1$) but also further-neighbor ones ($n > 1$), in close analogy to the well-established case of J_n [2]. A quadrupolar operator at site i, $\mathbf{Q}_i$, has five components: $Q_i^{x^2-y^2} = (S_i^x)^2 - (S_i^y)^2$, $Q_i^{3z^2-r^2} = [2(S_i^z)^2 - (S_i^x)^2 - (S_i^y)^2]/\sqrt{3}$, $Q^{xy} = S_i^x S_i^y + S_i^y S_i^x$, $Q^{yz} = S_i^y S_i^z + S_i^z S_i^y$, and $Q^{zx} = S_i^z S_i^x + S_i^x S_i^z$. The biquadratic term can be re-expressed as $(\mathbf{S}_i \cdot \mathbf{S}_j)^2 = (\mathbf{Q}_i \cdot \mathbf{Q}_j)/2 - (\mathbf{S}_i \cdot \mathbf{S}_j)/2 + (\mathbf{S}_i^2 \mathbf{S}_j^2)/3$.

It is convenient to choose the time-reversal invariant basis of the SU(3) fundamental representation [28, 32],

$$|x\rangle = \frac{i|1\rangle - i|\bar{1}\rangle}{\sqrt{2}}, \quad |y\rangle = \frac{|1\rangle + |\bar{1}\rangle}{\sqrt{2}}, \quad |z\rangle = -i|0\rangle, \quad (2)$$

where we abbreviate $|S^z = \pm 1\rangle \equiv |\pm 1\rangle$ ($|S^z = 0\rangle \equiv |0\rangle$) and $|\bar{1}\rangle \equiv |-1\rangle$. We can introduce a site-factorized wavefunction at each site to characterize any ordered state with short-ranged correlations as

$$|\mathbf{d}_i\rangle = d_i^x|x\rangle + d_i^y|y\rangle + d_i^z|z\rangle, \quad (3)$$

where $d_i^{x,y,z}$ are complex numbers and can be re-expressed in the vector form called director, $\mathbf{d}_i = (d_i^x,\ d_i^y,\ d_i^z)$, with the basis $\{|x\rangle,\ |y\rangle,\ |z\rangle\}$. We can then re-express the model Hamiltonian as [46]

$$H_{sf} = \sum_{i,\delta_n} \left[J_n \left| \mathbf{d}_i \cdot \bar{\mathbf{d}}_j \right|^2 + (K_n - J_n) \left| \mathbf{d}_i \cdot \mathbf{d}_j \right|^2 + K_n \right], \quad (4)$$

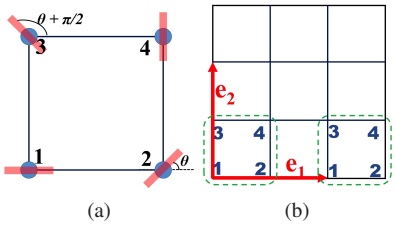

FIG. 2. (Color online) (a) Illustration of the $(\pi, 0)$ AFQ found within the site-factorized wave function studies. The red bars are the directors $\mathbf{d}$ labeling the quadrupolar direction. Generically, there are 4 sublattices per unit cell, and the two independent directors are specified by one independent angle θ. (b) Illustration of the square network consisting of the lattice for performing flavor-wave theory calculations. The unit cells, which contains 4 sublattices, are connected by the vectors $\mathbf{e}_1 \equiv \hat{x}$ and $\mathbf{e}_2 \equiv \hat{y}$, where we set the lattice constant $a \equiv 1$.

where the subscript "sf" refers to the site-factorized Hamiltonian. In the following, we will drop the irrelevant constant terms in Eq. (4). Within the SU(3) basis, the ferroquadrupolar phase (FQ) has all directors aligned along a particular direction. In contrast, in AFQ the directors at different sublattices are orthogonal to each other.

AFQ order from site-factorized wavefunction— We study the phase diagram using a variational method based on the site-factorized wave-functions on a $L \times L$ square lattice with L up to 6 and periodic boundary condition. We first illustrate our result by considering fixed $J_1 = J_2 = 1/4$, $J_3 = 0$ and $K_1 = -1$, and variable K_2 and K_3. (See below about the robustness of our result over an extended parameter range. As shown in Fig. 1, the ground state phase diagram contains four phases: a collinear AFM (CAFM) ordered at wave vectors $(\pi, 0)/(0, \pi)$, a Néel AFM ordered at (π, π), a FQ ordered at $(0, 0)$, and an AFQ ordered at $(\pi, 0)/(0, \pi)$. Within our approach, we did not find evidence for any three-sublattice AFQ order. [31–33]

Figure 2(a) illustrates the directors in the $(\pi, 0)$ AFQ, in which there are 4 sublattices. The $\mathbf{d}$ directors connected by the second-neighbor bonds are *mutually orthogonal* to each other, while the nearest-neighbor $\mathbf{d}$-s are subject to an angle θ. In the 4 sublattices, there are only 2 independent $\mathbf{d}$-s. We choose those sitting on sublattices 1 and 2 to be independent, which then specifies the $\mathbf{d}$-s on sites 3 and 4 straightforwardly due to orthogonality. This leads to the following parametrization for the $\mathbf{d}$-s:

$$\begin{aligned} \mathbf{d}_1 &= \begin{pmatrix} 1 & 0 & 0 \end{pmatrix}, & \mathbf{d}_2 &= \begin{pmatrix} \cos\theta & \sin\theta & 0 \end{pmatrix}, \\ \mathbf{d}_3 &= \begin{pmatrix} -\sin\theta & \cos\theta & 0 \end{pmatrix}, & \mathbf{d}_4 &= \begin{pmatrix} 0 & 1 & 0 \end{pmatrix}. \end{aligned} \quad (5)$$

Despite the finite angle between $\mathbf{d}_1$ and $\mathbf{d}_2$, the energy of $(\pi, 0)$ AFQ is *independent* of the angle θ within this semi-classical approach, which can be seen by plugging $\mathbf{d}$ directors into Eq. (4). Thus, the semiclassical $(\pi, 0)$ AFQ is *infinitely degenerate* at the level of site-factorized wavefunction studies, which *do not* include the quantum fluctuations. [Quantum fluctuations will lift the degeneracy (see below).] The bound-

aries between each phase can be determined analytically [46], which are consistent with the numerical results.

Quantum fluctuations stabilizing $(\pi,0)$ *AFQ*— The $(\pi,0)$ AFQ at the level of the site-factorized wave function is illustrated in Fig. 2(a), in which the angle θ varies between 0 and π. The states with angles $\theta=0$ or $\pi/2$ correspond to the AFQ state of interest, at wave vector $(0,\pi)$ or $(\pi,0)$, respectively. Below we study the effect of the quantum fluctuations in this AFQ using the flavor-wave theory formulation.

For the flavor wave calculation, we associate 3 Schwinger-bosons at each site i, $b_{i\alpha=x,y,z}$, to the states of Eq. (2), where $b^\dagger_{i\alpha}|vac\rangle = |\alpha\rangle$ with $|vac\rangle$ being the vacuum state of the Schwinger bosons. The bosons satisfy a local constraint $\sum_\alpha b^\dagger_{i\alpha}b_{i\alpha}=1$. The Hamiltonian, Eq. (1), can be rewritten as

$$H=\sum_{i,\delta_n,\alpha,\beta}\left[J_n b^\dagger_{i\alpha}b_{j\alpha}b^\dagger_{j\beta}b_{i\beta}+(K_n-J_n)\,b^\dagger_{i\alpha}b^\dagger_{j\alpha}b_{j\beta}b_{i\beta}\right] \quad (6)$$

Following the usual procedure of the spin-wave theory calculations, we introduce different local rotations around z-axis for each sublattice $i=1,2,3,4$ as $a_{i\alpha}=\sum_\beta\left(\mathcal{R}^{\theta_i}_z\right)_{\alpha\beta}b_{i\beta}$, where $\mathcal{R}^{\theta_i}_z$ represents the SO(3) matrix for a rotation around the z-axis by angles θ_i that are determined according to Eq. (5) and Fig. 2(a). At each site, we assume that only a_{ix} condenses, and we replace $a^\dagger_{ix}$ and a_{ix} by $(M-a^\dagger_{iy}a_{iy}-a^\dagger_{iz}a_{iz})^{1/2}$, where $M=1$ in the present case. A $1/M$ expansion up to the quadratic order in the bosons a_y and a_z followed by an appropriate Holstein-Primakoff transformation allows us to extract the ground state energy. From now on we replace the labeling $a_{i\alpha}=a_\alpha(\mathbf{r},a)$, where $\mathbf{r}$ runs over the Bravais lattice of unit cells of the square network and $a=1,2,3,4$ runs over the sub lattices, as illustrated in Fig. 2(b). The different unit cells are connected by $\mathbf{e}_1\equiv\hat{x}$ and $\mathbf{e}_2\equiv\hat{y}$.

For clarity, we introduce $D^T_\alpha(\mathbf{k})\equiv\{a_\alpha(\mathbf{k},1),a_\alpha(\mathbf{k},2),a_\alpha(\mathbf{k},3),a_\alpha(\mathbf{k},4)\}$ and $A^T_\alpha(\mathbf{k})\equiv\left\{D^T_\alpha(\mathbf{k}),D^\dagger_\alpha(-\mathbf{k})\right\}$, where $\alpha=y,z$. We arrange the Hamiltonian [47] to be $H=\mathcal{H}_c+\mathcal{H}_B$. The first term, $\mathcal{H}_c=8\sum_k\Big[J_1+K_1+J_2\left(1-\sin^2(2\theta)/8\right)-K_2+J_3\left(1-\sum_{\mu=1,2}\cos(\mathbf{k}\cdot\mathbf{e}_\mu)+\sin^2(2\theta)/8\right)+3K_3\Big]$, represents the semiclassical ground-state energy. The second term $\mathcal{H}_B$ is expressed as $\mathcal{H}_B=\sum_{\mathbf{k},\eta=y,z}A^\dagger_\eta\mathcal{H}_\eta A_\eta$, with

$$\mathcal{H}_\eta=\begin{pmatrix}\alpha_\eta & \gamma_\eta\\ \gamma^\dagger_\eta & \alpha_\eta\end{pmatrix}, \quad (7)$$

where α_η and γ_η are 4×4 Hermitian matrices and are functions of momenta $\mathbf{k}$, couplings J_n and K_n, and the angle θ. $\mathcal{H}_B$ contains the zero-point energy of the boson fields, which plays the role of quantum correction to the semiclassical ground-state energy. We leave the full expressions of the matrices to the Supplemental Material [46].

Figure 3 shows the ground state energy of the $(\pi,0)$ AFQ vs θ within the flavor-wave theory at $\{K_2,K_3\}=\{1,-1\}$. The two degenerate quadrupolar ground states at $\theta=0,\pi/2$ correspond to the AFQ with the ordering wavevector $(\pi,0)$ or $(0,\pi)$. We conclude that the quantum fluctuations lift the infinite degeneracy and stabilize the $(\pi,0)$ AFQ.

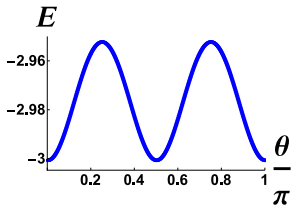

FIG. 3. (Color online) Energy per site of the $(\pi,0)$ AFQ vs θ obtained in the flavor-wave theory calculations. The system we use in the numerics consists of 100×100 unit cells, with 4 sites per unit cell. The parameters for this calculation are $(K_2,K_3)=(1,-1)$.

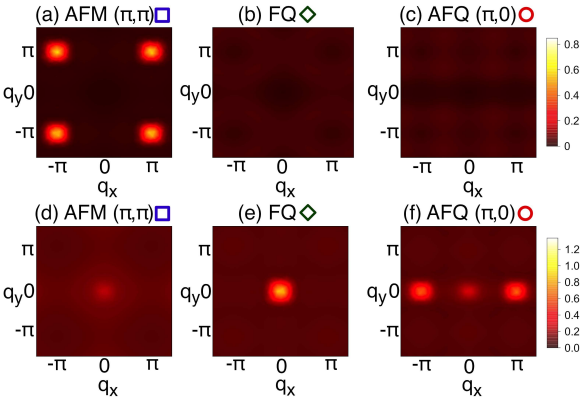

FIG. 4. (Color online) The spin dipolar ((a)-(c)) and quadrupolar ((d)-(f)) structure factors, $m^2_s(\mathbf{q})$ and $m^2_Q(\mathbf{q})$, with $(J_1,J_2,J_3,K_1)=(1/4,1/4,0,-1)$ on $L_y=8$ lattice for Néel order [(a)/(d)] with $(K_2,K_3)=(1,1)$), FQ [(b)/(e)] with $(K_2,K_3)=(-1,-1)$, and $(\pi,0)$ AFQ [(c)/(f)] with $(K_2,K_3)=(1,-1)$. The color represents the peak height of the corresponding structure factor.

Density Matrix Renormalization Group Analysis— To further demonstrate the stability of the $(\pi,0)$ AFQ phase and to analyze the GBQ model in an unbiased way, we turn next to the study of the ground states using the SU(2) DMRG calculations [40, 48–51]. To search for the $(\pi,0)$ AFQ order, we specifically consider the parameter point, $(K_2,K_3)=(1,-1)$, where the $(\pi,0)$ AFQ is realized in Fig. 1 (recall $J_1=J_2=1/4$ and $K_1=-1$). For comparison, we also consider two parameter points in the nearby regimes, $(K_2,K_3)=(-1,-1)$ and $(1,1)$, corresponding to the FQ and Néel AFM, respectively, in Fig. 1 (the other parameters are unchanged). We perform DMRG simulations on cylindrical geometries with $L_y=6,8$ lattice spacings keeping up to 6000 SU(2) states and $L_y=10$ keeping up to 4000 SU(2) states. We rescale the parameters with respect to J_1. The largest truncation errors are around 10^{-5}. Especially on the $L_y=10$ cylinder, we have checked the results corresponding to 2000 and 4000 SU(2) states, and found the differences to be small (around 10^{-3}) for m^2_S and m^2_Q.

We choose $L_y=L$ to calculate the spin ($\langle\mathbf{S}_i\cdot\mathbf{S}_j\rangle$) and

quadrupolar ($\langle \mathbf{Q}_i \cdot \mathbf{Q}_j \rangle$) correlation functions in the middle of $L \times 2L$ cylinder systems to obtain the corresponding structure factors [49, 51], $m_S^2(\mathbf{q}) \equiv (1/L^4) \sum_{ij} \langle \mathbf{S}_i \cdot \mathbf{S}_j \rangle e^{i\mathbf{q}\cdot(\mathbf{r}_i - \mathbf{r}_j)}$ and $m_Q^2(\mathbf{q}) \equiv (1/L^4) \sum_{ij} \langle \mathbf{Q}_i \cdot \mathbf{Q}_j \rangle e^{i\mathbf{q}\cdot(\mathbf{r}_i - \mathbf{r}_j)}$, in Figs. 4(a)-(f). We obtain the results at parameter points $(K_2, K_3) = (1, 1)$, $(-1, -1)$, and $(1, -1)$ shown, respectively, in Figs. 4[(a)/(d)], [(b)/(e)], and [(c)/(f)]. Fig. 4[(a)/(d)] show a sharp peak at $(\pm\pi, \pm\pi)$ in $m_S^2(\mathbf{q})$ and a weak FQ peak at $(0, 0)$ in $m_Q^2(\mathbf{q})$ suggesting the Néel AFM. We note that for spin-1 system the magnetically-ordered states are expected to show finite FQ order. Fig. 4[(b)/(e)] show no magnetic order signature in $m_S^2(\mathbf{q})$ and a sharp peak at $(0, 0)$ in $m_Q^2(\mathbf{q})$ suggesting the ground state is FQ. Fig. 4[(c)/(f)] show no clear signature in $m_S^2(\mathbf{q})$ and sharp peaks at $(\pm\pi, 0)$ in $m_Q^2(\mathbf{q})$ suggesting the realization of the $(\pi, 0)$ AFQ, which is confirmed under finite-size scaling analysis. [46] We note that Fig. 4(f) also shows a peak at $\mathbf{q} = (0, 0)$ in $(\pi, 0)$ AFQ. This is theoretically expected: For a two-sublattice AFQ order at $(\pi, 0)$, one diagonal component of the quadrupolar operator $Q^{x^2-y^2}$ takes staggered values at sublattices A and B, $\langle Q_i^{x^2-y^2} \rangle = \langle (S_i^x)^2 \rangle - \langle (S_i^y)^2 \rangle = (-1)^i$, which implies $\langle (S_i^x)^2 \rangle = \delta_{iA}$ and $\langle (S_i^y)^2 \rangle = \delta_{iB}$; correspondingly, the other diagonal component takes *uniform* expectation values at each site, $\langle Q_i^{3z^2-r^2} \rangle = -1/\sqrt{3}$, and thus shows the FQ peak.

Discussions— We close by remarking on several points. First, both our analytical and numerical calculations indicate that the $(\pi, 0)$ AFQ order is not accompanied by any AFM order.

Second, the $(\pi, 0)$ AFQ ground state is stable over a very wide range in the parameter space. To illustrate this point, we consider the case of $-K_1/J_2 = 0.8$, which is expected to be realistic to FeSe since it is already close to that extracted from fitting the spin spectra of related iron-based systems [43]. Continuing to set $J_1 = J_2 = 1/4$, and taking $K_2 = -K_3 = -K_1 = 1/5$, we show that the $(\pi, 0)$ AFQ ground state persists (see the Supplemental Material; particularly, Fig. S3) [46].

Third, the $(\pi, 0)$ AFQ state breaks the C_4 symmetry, and associated with it is an Ising-nematic order. The latter is expected to be dominated by the following order parameter [18]:

$$\sigma_2 = \sum_i \left[(\mathbf{S}_i \cdot \mathbf{S}_{i+\hat{x}})^2 - (\mathbf{S}_i \cdot \mathbf{S}_{i+\hat{y}})^2 \right]. \tag{8}$$

While this is clearly the case for the ground state, σ_2 will persist at nonzero temperatures even in the purely two-dimensional limit. (In the presence of an interlayer coupling, the AFQ order will also extent to nonzero temperatures.) This provides the basis to understand the nematic transition at T_s in FeSe.

Fourth, in a $(\pi, 0)$ AFQ state, the low-energy spin excitations are expected to be concentrated near the wavevector $(\pi, 0)$. The spectral weight at low energies should be linear in ω [18]: It is proportional to $[M(\omega)]^2/\omega$, with the spectral weight of the quadrupolar Goldstone mode *per se* contributing the factor $1/\omega$, and the spin dipolar matrix element of the quadrupolar mode $M(\omega)$ being $\propto \omega$. (This argument is valid for any AFQ order at zero magnetic field and, indeed, the linear-in-ω dependence also appears in the three-sublattice $(2\pi/3, 2\pi/3)$ AFQ state on the triangular lattice [34].) Such a linear dependence has been observed (up to about 50 meV) by the recent neutron-scattering experiments in FeSe[23, 24]. At higher energies, the spin excitations are expected to spread over a large range of wavevectors, including a sizable spectral weight near (π,π). This is also consistent with the neutron-scattering measurements in FeSe [23, 24].

Finally, the quadrupolar operator acts like a spin-2 operator. Thus, in the absence of spin-orbit coupling, the AFQ order parameter cannot be coupled to the bilinear fermion fields. (In the Supplemental Material [46], the result is derived from a rigorous group-symmetry analysis.) This implies that the AFQ order does not reconstruct the Fermi surface. Instead, the coupling to the bilinears of the itinerant electrons is only through the nematic order parameter, which induces a distortion of the Fermi surface. In contrast to what happens above the ordering temperature, the Fermi surface in the AFQ state will lose the invariance under a C_4-rotation: *e.g.*, the hole Fermi pockets near Γ will be elongated along one of the axis directions. All these features are consistent with the observations of photoemission experiments[15], when twin domains are taken into account.

Acknowledgement– We would like to acknowledge useful discussions with Shoushu Gong and Zhentao Wang. We thank Zhentao Wang for providing the codes for site-factorized wavefunction studies and Shoushu Gong for providing the SU(2) DMRG code. This work was supported in part by the NSF Grant No. DMR-1611392 and the Robert A. Welch Foundation Grant No. C-1411 (H-H.L., W-J.H. and Q.S.), by the NSF Grant No. DMR-1350237 (H-H. L. and W-J.H.), by a Smalley Postdoctoral Fellowship in Rice Center for Quantum Materials (H-H. L.), and by the National Science Foundation of China Grant number 11374361 and the Fundamental Research Funds for the Central Universities and the Research Funds of Renmin University of China (R.Y.). The majority of the computational calculations have been performed on the Shared University Grid at Rice funded by NSF under Grant EIA-0216467, a partnership between Rice University, Sun Microsystems, and Sigma Solutions, Inc., the Big-Data Private-Cloud Research Cyber-infrastructure MRI-award funded by NSF under Grant No. CNS-1338099, the Extreme Science and Engineering Discovery Environment (XSEDE) by NSF under Grants No. DMR160003.

[1] Y. Kamihara, T. Watanabe, M. Hirano, and H. Hosono, Journal of the American Chemical Society **130**, 3296 (2008).

[2] Q. Si, R. Yu, and E. Abrahams, Nature Reviews Materials **1**, 16017 (2016).

[3] W. Qing-Yan, L. Zhi, Z. Wen-Hao, Z. Zuo-Cheng, Z. Jin-Song, L. Wei, D. Hao, O. Yun-Bo, D. Peng, C. Kai, W. Jing, S. Can-Li, H. Ke, J. Jin-Feng, J. Shuai-Hua, W. Ya-Yu, W. Li-Li,

C. Xi, M. Xu-Cun, and X. Qi-Kun, Chinese Physics Letters **29**, 037402 (2012).
[4] J. J. Lee, F. T. Schmitt, R. G. Moore, S. Johnston, Y.-T. Cui, W. Li, M. Yi, Z. K. Liu, M. Hashimoto, Y. Zhang, D. H. Lu, T. P. Devereaux, D.-H. Lee, and Z.-X. Shen, Nature **515**, 245 (2014).
[5] S. He, J. He, W. Zhang, L. Zhao, D. Liu, X. Liu, D. Mou, Y.-B. Ou, Q.-Y. Wang, Z. Li, L. Wang, Y. Peng, Y. Liu, C. Chen, L. Yu, G. Liu, X. Dong, J. Zhang, C. Chen, Z. Xu, X. Chen, X. Ma, Q. Xue, and X. J. Zhou, Nat Mater **12**, 605 (2013).
[6] Z. Zhang, Y.-H. Wang, Q. Song, C. Liu, R. Peng, K. A. Moler, D. Feng, and Y. Wang, Science Bulletin **60**, 1301 (2015).
[7] F.-C. Hsu, J.-Y. Luo, K.-W. Yeh, T.-K. Chen, T.-W. Huang, P. M. Wu, Y.-C. Lee, Y.-L. Huang, Y.-Y. Chu, D.-C. Yan, and M.-K. Wu, Proceedings of the National Academy of Sciences **105**, 14262 (2008).
[8] M. H. Fang, H. M. Pham, B. Qian, T. J. Liu, E. K. Vehstedt, Y. Liu, L. Spinu, and Z. Q. Mao, Phys. Rev. B **78**, 224503 (2008).
[9] T. M. McQueen, A. J. Williams, P. W. Stephens, J. Tao, Y. Zhu, V. Ksenofontov, F. Casper, C. Felser, and R. J. Cava, Phys. Rev. Lett. **103**, 057002 (2009).
[10] S. Medvedev, T. M. McQueen, I. A. Troyan, T. Palasyuk, M. I. Eremets, R. J. Cava, S. Naghavi, F. Casper, V. Ksenofontov, G. Wortmann, and C. Felser, Nat Mater **8**, 630 (2009).
[11] A. E. Böhmer, T. Arai, F. Hardy, T. Hattori, T. Iye, T. Wolf, H. v. Löhneysen, K. Ishida, and C. Meingast, Phys. Rev. Lett. **114**, 027001 (2015).
[12] S.-H. Baek, D. V. Efremov, J. M. Ok, J. S. Kim, J. van den Brink, and B. Bchner, Nat Mater **14**, 210 (2015).
[13] K. Nakayama, Y. Miyata, G. N. Phan, T. Sato, Y. Tanabe, T. Urata, K. Tanigaki, and T. Takahashi, Phys. Rev. Lett. **113**, 237001 (2014).
[14] T. Shimojima, Y. Suzuki, T. Sonobe, A. Nakamura, M. Sakano, J. Omachi, K. Yoshioka, M. Kuwata-Gonokami, K. Ono, H. Kumigashira, A. E. Böhmer, F. Hardy, T. Wolf, C. Meingast, H. v. Löhneysen, H. Ikeda, and K. Ishizaka, Phys. Rev. B **90**, 121111 (2014).
[15] M. D. Watson, T. K. Kim, A. A. Haghighirad, N. R. Davies, A. McCollam, A. Narayanan, S. F. Blake, Y. L. Chen, S. Ghannadzadeh, A. J. Schofield, M. Hoesch, C. Meingast, T. Wolf, and A. I. Coldea, Phys. Rev. B **91**, 155106 (2015).
[16] T. Terashima, N. Kikugawa, S. Kasahara, T. Watashige, T. Shibauchi, Y. Matsuda, T. Wolf, A. E. Bhmer, F. Hardy, C. Meingast, H. v. Lhneysen, and S. Uji, Journal of the Physical Society of Japan **84**, 063701 (2015).
[17] P. Dai, Rev. Mod. Phys. **87**, 855 (2015).
[18] R. Yu and Q. Si, Phys. Rev. Lett. **115**, 116401 (2015).
[19] F. Wang, S. A. Kivelson, and D.-H. Lee, Nat Phys **11**, 959 (2015).
[20] J. K. Glasbrenner, I. I. Mazin, H. O. Jeschke, P. J. Hirschfeld, R. M. Fernandes, and R. Valenti, Nat Phys **11**, 953 (2015).
[21] M. C. Rahn, R. A. Ewings, S. J. Sedlmaier, S. J. Clarke, and A. T. Boothroyd, Phys. Rev. B **91**, 180501 (2015).
[22] Q. Wang, Y. Shen, B. Pan, Y. Hao, M. Ma, F. Zhou, P. Steffens, K. Schmalzl, T. R. Forrest, M. Abdel-Hafiez, X. Chen, D. A. Chareev, A. N. Vasiliev, P. Bourges, Y. Sidis, H. Cao, and J. Zhao, Nat Mater **15**, 159 (2016).
[23] Q. Wang, Y. Shen, B. Pan, X. Zhang, K. Ikeuchi, K. Iida, A. D. Christianson, H. C. Walker, D. T. Adroja, M. Abdel-Hafiez, X. Chen, D. A. Chareev, A. N. Vasiliev, and J. Zhao, Nat Commun **7**, 12182 (2016).
[24] S. Shamoto, K. Matsuoka, R. Kajimoto, M. Ishikado, Y. Yamakawa, T. Watashige, S. Kasahara, M. Nakamura, H. Kontani, T. Shibauchi, and Y. Matsuda, arXiv:1511.04267 (unpublished).
[25] M. Blume and Y. Y. Hsieh, Journal of Applied Physics **40**, 1249 (1969).
[26] H. H. Chen and P. M. Levy, Phys. Rev. Lett. **27**, 1383 (1971).
[27] A. F. Andreev and I. A. Grishchuk, JETP **60**, 268 (1984).
[28] N. Papanicolaou, Nuclear Physics B **305**, 367 (1988).
[29] N. Shannon, T. Momoi, and P. Sindzingre, Phys. Rev. Lett. **96**, 027213 (2006).
[30] A. Läuchli, F. Mila, and K. Penc, Phys. Rev. Lett. **97**, 087205 (2006).
[31] T. A. Tóth, A. M. Läuchli, F. Mila, and K. Penc, Phys. Rev. Lett. **105**, 265301 (2010).
[32] T. A. Tóth, A. M. Läuchli, F. Mila, and K. Penc, Phys. Rev. B **85**, 140403 (2012).
[33] B. Bauer, P. Corboz, A. M. Läuchli, L. Messio, K. Penc, M. Troyer, and F. Mila, Phys. Rev. B **85**, 125116 (2012).
[34] A. Smerald and N. Shannon, Phys. Rev. B **88**, 184430 (2013).
[35] A. Smerald, H. T. Ueda, and N. Shannon, Phys. Rev. B **91**, 174402 (2015).
[36] H.-H. Lai, Phys. Rev. B **87**, 205131 (2013).
[37] H.-H. Lai, Phys. Rev. B **87**, 205111 (2013).
[38] C. L. Henley, Phys. Rev. Lett. **62**, 2056 (1989).
[39] P. Chandra, P. Coleman, and A. I. Larkin, Phys. Rev. Lett. **64**, 88 (1990).
[40] S. R. White, Phys. Rev. Lett. **69**, 2863 (1992).
[41] S. R. White, Phys. Rev. B **48**, 10345 (1993).
[42] X. Zhang, M. Bishof, S. L. Bromley, C. V. Kraus, M. S. Safronova, P. Zoller, A. M. Rey, and J. Ye, Science **345**, 1467 (2014).
[43] R. Yu, Z. Wang, P. Goswami, A. H. Nevidomskyy, Q. Si, and E. Abrahams, Phys. Rev. B **86**, 085148 (2012).
[44] A. L. Wysocki, K. D. Belashchenko, and V. P. Antropov, Nat Phys **7**, 485 (2011).
[45] P. Fazekas, *Lecture Notes on Electron Correlation and Magnetism (Series in Modern Condensed Matter Physics)* (Singapore etc. : World Scientific, 1999).
[46] See Supplemental Material [url], which includes Refs. [52–58].
[47] M.-w. Xiao, arXiv:0908.0787v1 (unpublished).
[48] I. McCulloch and M. Gulácsi, Europhysics Letters **57**, 852 (2002).
[49] S.-S. Gong, W. Zhu, D. N. Sheng, O. I. Motrunich, and M. P. A. Fisher, Phys. Rev. Lett. **113**, 027201 (2014).
[50] S.-S. Gong, W. Zhu, and D. Sheng, Scientific reports **4**, 6317 (2014).
[51] S.-S. Gong, D. N. Sheng, O. I. Motrunich, and M. P. A. Fisher, Phys. Rev. B **88**, 165138 (2013).
[52] J. F. Cornwell, *Group Theory in Physics, Vol. I* (Academic Press, Cambridge, MA, 1986).
[53] J. F. Cornwell, *Group Theory in Physics, Vol. II* (Academic Press, Cambridge, MA, 1997).
[54] R. Shiina, H. Shiba, and P. Thalmeier, Journal of the Physical Society of Japan **66**, 1741 (1997).
[55] M. Bendele, A. Amato, K. Conder, M. Elender, H. Keller, H.-H. Klauss, H. Luetkens, E. Pomjakushina, A. Raselli, and R. Khasanov, Phys. Rev. Lett. **104**, 087003 (2010).
[56] M. Bendele, A. Ichsanow, Y. Pashkevich, L. Keller, T. Strässle, A. Gusev, E. Pomjakushina, K. Conder, R. Khasanov, and H. Keller, Phys. Rev. B **85**, 064517 (2012).
[57] T. Imai, K. Ahilan, F. L. Ning, T. M. McQueen, and R. J. Cava, Phys. Rev. Lett. **102**, 177005 (2009).
[58] Z. Xu, J. A. Schneeloch, J. Wen, E. S. Božin, G. E. Granroth, B. L. Winn, M. Feygenson, R. J. Birgeneau, G. Gu, I. A. Zaliznyak, J. M. Tranquada, and G. Xu, Phys. Rev. B **93**, 104517

(2016).